MIT Open Access Articles

Phage-Assisted Evolution of Bacillus methanolicus Methanol Dehydrogenase 2

Phage-Assisted Evolution of *Bacillus methanolicus* Methanol Dehydrogenase 2

Timothy B. Roth,[†,‡,§,#] Benjamin M. Woolston,[‖,#] Gregory Stephanopoulos,[‖] and David R. Liu*,[†,‡,§]

†Merkin Institute of Transformative Technologies in Healthcare, Broad Institute of MIT and Harvard, Cambridge, Massachusetts 02142, United States

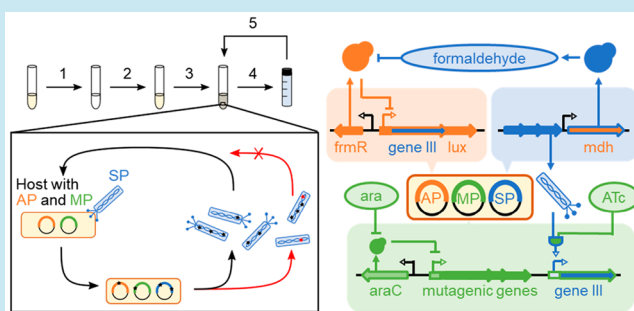‡Howard Hughes Medical Institute, Harvard University, Cambridge, Massachusetts 02138, United States

§Department of Chemistry and Chemical Biology, Harvard University, Cambridge, Massachusetts 02138, United States

‖Department of Chemical Engineering, Massachusetts Institute of Technology, Cambridge, Massachusetts 02139, United States

S *Supporting Information*

ABSTRACT: Synthetic methylotrophy, the modification of organisms such as *E. coli* to grow on methanol, is a longstanding goal of metabolic engineering and synthetic biology. The poor kinetic properties of NAD-dependent methanol dehydrogenase, the first enzyme in most methanol assimilation pathways, limit pathway flux and present a formidable challenge to synthetic methylotrophy. To address this bottleneck, we used a formaldehyde biosensor to develop a phage-assisted noncontinuous evolution (PANCE) selection for variants of *Bacillus methanolicus* methanol dehydrogenase 2 (Bm Mdh2). Using this selection, we evolved Mdh2 variants with up to 3.5-fold improved V_{max}. The mutations responsible for enhanced activity map to the predicted active site region homologous to that of type III iron-dependent alcohol dehydrogenases, suggesting a new critical region for future methanol dehydrogenase engineering strategies. Evolved Mdh2 variants enable twice as much ^{13}C-methanol assimilation into central metabolites than previously reported state-of-the-art methanol dehydrogenases. This work provides improved Mdh2 variants and establishes a laboratory evolution approach for metabolic pathways in bacterial cells.

KEYWORDS: *methanol dehydrogenase, synthetic methylotrophy, methanol assimilation, directed evolution, phage-assisted continuous evolution, phage-assisted noncontinuous evolution*

Protein evolution and engineering have improved a wide range of enzymes relevant to biotechnology. Phage-assisted continuous evolution (PACE) and phage-assisted noncontinuous evolution (PANCE) enable rapid protein evolution without regular researcher intervention and have been used to rapidly evolve a wide variety of phenotypes that impact protein synthesis or degradation,[1−4] protein and DNA binding,[5−7] or transcription.[8−10] To date, no PACE or PANCE selections have been described that evolve enzymes that biosynthesize small molecules. The evolution of such enzymes poses unique challenges due to the limited range of available biosensors that link the small molecules to a selectable or screenable output,[11] the challenge of evolving complex or non-native biosynthetic transformations, and the large size of many biosynthetic gene clusters.[12] Despite these challenges, the ability to evolve enzymes that mediate small-molecule biosynthesis has the potential to advance industrial production of important industrial compounds and drug precursors,[13] processing of waste products such as cellulosic biomass and methane, and other important biosynthetic processes.

Methane is a compelling target for microbial and enzymatic conversion given its cost effectiveness compared to other feedstocks such as glucose.[14] Naturally occurring microbial communities are capable of using methane as a sole carbon source, raising the possibility of using microbial engineering to better harness this resource.[15] However, methane is expensive to transport and contributes significantly to global warming.[16] A popular strategy for removing excess methane is wasteful combustion into carbon dioxide, a less potent greenhouse gas.[17] Developing methods to transform this single-carbon resource into higher molecular weight products through biorefining could provide a less harmful and wasteful route to processing methane.[18,19] Methane oxidation yields methanol, which can be fermented by bacteria into higher-value products.[18,20,21] Engineering microbes to assimilate methanol more efficiently is thus an attractive stepping-stone to the bioconversion of methane into commodity chemicals.[14]
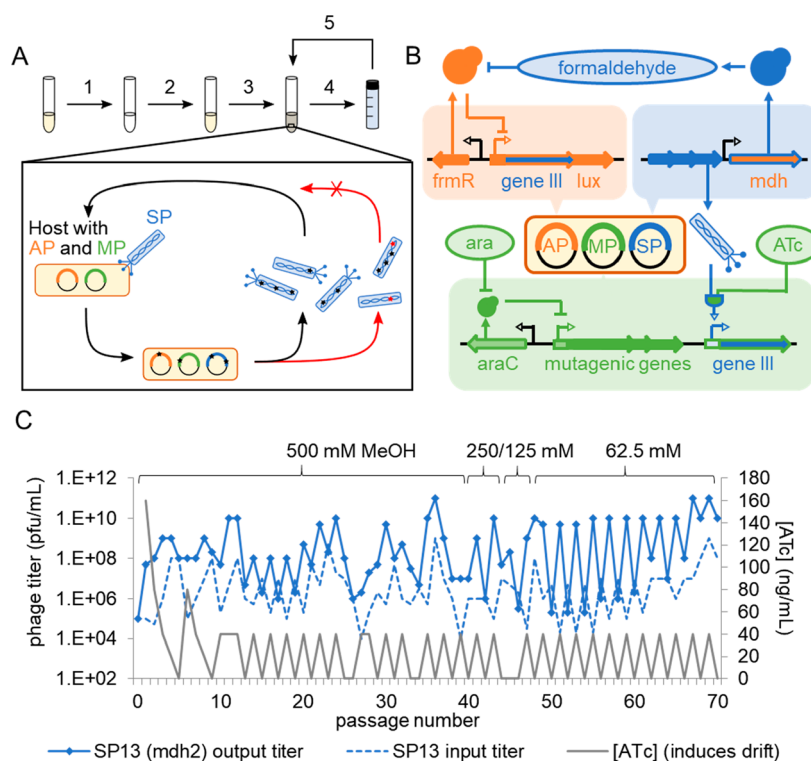
Figure 1. Phage assisted noncontinuous evolution of methanol dehydrogenase. (A) General procedure for PANCE. Starting from a saturated, overnight culture of host cells containing the accessory plasmid (AP) and mutagenesis Plasmid (MP), cultures are (1) diluted; (2) grown to log-phase; (3) infected with selection phage (SP) and treated with desired inputs (*e.g.*, methanol, arabinose, ATc, glutathione); and (4) grown overnight and isolated the next day as a new population of SP; before (5) infecting a fresh log-phase host cell culture. In the selection circuit, black stars represent permissive and beneficial mutations, and red stars represent detrimental mutations. (B) The selection circuit for evolving methanol dehydrogenase genes in PANCE. Phage-associated genes are shown in blue, genes related to mdh activity are shown in orange, and genes relating to mutagenesis and drift regulation are shown in green. "ara" = arabinose. (C) Phage titers, dilution rates, and selection conditions for a single, 2 mL culture of a Selection Phage encoding *B. methanolicus mdh2* evolved for 70 passages in total.

A variety of methylotrophic microbes that can grow on methanol as their sole carbon source assimilate methanol into central metabolism through oxidation of methanol by a methanol dehydrogenase (Mdh) enzyme. The resulting formaldehyde is then funneled into one of two assimilation pathways: the ribulose monophosphate (RuMP) pathway[22] or the serine cycle.[23] Engineering native methylotrophs directly to both consume methanol and convert it into high-value products poses a significant challenge due to limited information and biochemical techniques available for modifying these organisms.[24,25] While tools are in development to manipulate organisms such as *Methylobacterium extorquens*,[26−28] a promising alternative is to develop synthetic methylotrophy in model organisms such as *Escherichia coli* that are natively incapable of growing on methanol.[29] The RuMP pathway is an attractive choice for engineering synthetic methylotrophy in *E. coli* given its higher theoretical yield and greater compatibility with *E. coli* metabolism compared to the serine cycle.[22] Expressing an NAD-dependent methanol or alcohol dehydrogenase along with hexulose-6-phosphate synthase (Hps) and 6-phospho-3-hexuloisomerase (Phi) from native methylotrophs is sufficient to incorporate carbon from methanol feedstocks into *E. coli* central metabolism,[30] but still falls far short of enabling *E. coli* to use methanol as an exclusive carbon source. Further engineering to improve ribulose-5-phosphate regeneration can enable methanol-dependent growth, but requires gluconate to be fed as a cosubstrate.[31] The poor activity of methanol dehydrogenase enzymes,[32]

which typically exhibit millimolar K_m values, low catalytic rates, and a preference for oxidizing other alcohols, is considered a key barrier to enabling *E. coli* to use methanol as its sole carbon source.[32−35] Alternative methanol dehydrogenases such as those from *M. extorquens* use pyrroloquinoline quinone (PQQ) as a cofactor, which is not natively synthesized by *E. coli*.[30] As a result, identifying and engineering improved NAD(P)-dependent Mdh variants that can oxidize methanol more selectively, more efficiently, or in a manner that results in greater assimilation of methanol represents a major aspiration of developing synthetic methylotrophy in *E. coli*.[32]

A variety of NAD-dependent Mdh enzymes have been isolated, characterized, and evolved.[33,34,36] The Mdh2 enzyme from *Cupriavidus necator* was engineered for improved kinetics using a combination of *in vitro* library generation, automated colony picking, and a plate-based screen for formaldehyde production.[36] On the basis of reported *in vitro* kinetic parameters, this evolved Cn Mdh2 CT4−1 enzyme represents the state-of-the-art for methanol assimilation pathways in *E. coli*.[36,37] However, colony picking only screens several thousand variants per generation of evolution, in contrast with the mutational diversity sampled in selections such as PACE, which can process >10⁹ variants per phage generation (as short as 10 min).[8]

To test the ability of PACE to evolve improved Mdh variants, we first developed an *in vivo* selection that links methanol oxidation to phage propagation. We used this selection in a series of PANCE and PACE experiments to

evolve several Mdh variants with improved kinetic properties that assimilate approximately twice as much methanol as the previously reported state-of-the-art Cn Mdh2 CT4−1 enzyme. Our findings also inform future Mdh engineering efforts by identifying a critical region of mutations that impact Mdh activity and methanol assimilation near the predicted active site of *B. methanolicus* Mdh2 (Bm Mdh2).

■ RESULTS

Design and Characterization of Mdh PANCE. PACE and PANCE are laboratory evolution systems that couple a target phenotype to the life cycle of M13 filamentous bacteriophage. Gene III, required for phage propagation, is replaced on the phage genome with the gene(s) of interest, creating selection phage (SP) that are unable to propagate on their own. Host *E. coli* cells are engineered to contain a copy of gene III on an accessory plasmid (AP), which links gene III expression to the desired target gene function. SP propagate only if their evolving gene(s) possess the desired activity, thereby activating gene III expression on the AP. Fresh host cells continuously (PACE) or periodically (PANCE) dilute a fixed-volume vessel called the "lagoon" that contains the evolving SP population.[8] Library diversity is generated in cells using a mutagenesis plasmid (MP),[38] eliminating the need for *in vitro* library construction.

To apply PACE and PANCE to Mdh, we constructed an AP with gene III downstream of an optimized P_{frm} promoter.[37] The P_{frm} promoter and its corresponding regulator, FrmR, allow gene transcription only in the presence of formaldehyde, thereby linking gene III expression to conversion of methanol to formaldehyde by functional Mdh variants[39] (Figure 1A). Formaldehyde reacts irreversibly with a key cysteine residue of the FrmR repressor protein, releasing it from its cognate promoter sequence and permitting recruitment of the *E. coli* σ^{70} factor. In this manner, the concentration of formaldehyde determines the relative amount of transcription from this promoter based on the ratio of active to inactive FrmR present in the cell. We constructed a corresponding selection phage (SP) in which gene III in the M13 phage genome was replaced with the *mdh2* gene from *B. methanolicus* MGA3.[33] To avoid cross-talk between infected cells producing differing amounts of formaldehyde, we added glutathione to the growth media, which we previously showed acts as an extracellular formaldehyde sink to prevent cell-to-cell formaldehyde diffusion[37] (Figure 1A).

Phage propagation rates were initially too low to support evolution in a continuous flow system, even when using formaldehyde-sensitized S1030 Δ*frmA* host cells that lack the full detoxification pathway needed to convert formaldehyde into formate.[37] Nevertheless, Mdh2-mediated gene III expression was sufficient to support phage-assisted non-continuous evolution (PANCE)[4] (Figure 1B). The PANCE system uses iterative rounds of overnight phage propagation in discrete cultures of host cells and phage, instead of a continuous-flow lagoon (Figure 1A), allowing more stable monitoring, lower selection stringency, and maintenance of evolving phage populations since phage are only lost upon periodic dilution into fresh media with host cells. Upon addition of SP to cultures containing host *E. coli* with an AP and MP, SP expressing functional variants of Mdh will trigger gene III expression *via* FrmR on the AP, enabling the production of infectious progeny phage that can persist through multiple rounds of infection and replication. After

12−18 h, we isolated phage from the culture and passaged a small aliquot (2 to 200 μL) into a fresh culture of host cells (2 mL) to prevent the accumulation of mutations in the *E. coli* genome that could interfere with the evolution.

We adjusted the stringency of Mdh PANCE by changing both the amount of phage added from the previous passage and the amount of methanol added after phage addition. (Figure 1). We used an ATc-inducible phage shock promoter (PSP)[9] upstream of a second copy of gene III to periodically bypass the need to express gene III in response to Mdh activity. These periods of minimal selection stringency (evolutionary drift) allowed gene populations to diversify and expand between periods of more stringent selection conditions. We found that alternating between selection phases and ATc-induced "drift-phases" maintained a stable, high-titer phage population of *mdh*-encoding SP and prevented the gradual loss of SP populations that occurred when drift phases were not included (Figure 1C). Because the process of measuring phage population size takes a cycle of overnight growth, the actual number of phage (measured as plaque-forming units, pfu) used to infect each round was variable. Nevertheless, we never infected with fewer than 10^4 pfu for any given PANCE round using this approach (Figure 1C). Starting at passage 10 we also seeded fresh host cell cultures with a negative control SP encoding an enzyme with an unrelated biosynthetic function (*phaC* from *C. necator*[40]). This negative control population failed to persist during PANCE selection conditions despite always being passaged with the least stringent dilution rate between rounds (200 μL of added phage). Together, these results demonstrate that SP lacking Mdh activity, even with periodic drift, were lost over successive PANCE rounds (Figure S1).

Sequencing data across 70 overnight PANCE passages of Bm Mdh2 showed strong enrichment of M163V (Figure S2). This position is adjacent to A164, the amino acid homologous to the critical mutated A169 that was discovered during the evolution of Cn mdh2 CT4−1.[33,36] We subcloned several genes from sequenced individuals at intermediate passages and assayed these variants using a FrmR-mediated luciferase reporter system[37] (Figure S2). The assay results revealed that three representative individuals from passages 38 and 45 all increased apparent activity relative to wild-type Bm Mdh2 by 20 to 50-fold, with the M163V mutation on its own improving luciferase signal by over 30-fold, consistent with its proximity to A169 in Cn Mdh2. These findings suggest that M163V greatly improves apparent Mdh2 activity, consistent with its prevalence across all 70 PANCE passages.

Multiplexed Plate-Based PANCE of Bm Mdh2. Having demonstrated that an Mdh2-encoding phage can propagate in a 2 mL culture undergoing alternating drift and selection phases, we next sought to expand the throughput of PANCE by using 0.5 mL populations cultured in 96-well plates. We evolved populations of Bm Mdh2 SP in triplicate across six different concentrations of methanol, totaling 18 separate evolving populations. All passages were evolved using common dilution rates (0.5−50 μL) and alternating drift schedules designed to mimic the first experiment (Figure S3). We performed this plate-based PANCE for 40 passages (counting each drift or selection phase as a separate, numbered passage) without changing methanol concentrations. After passage 38 we analyzed remaining phage population size in each well and found that only populations fed 250 mM or 500 mM methanol persisted at high titers (Figure S3).
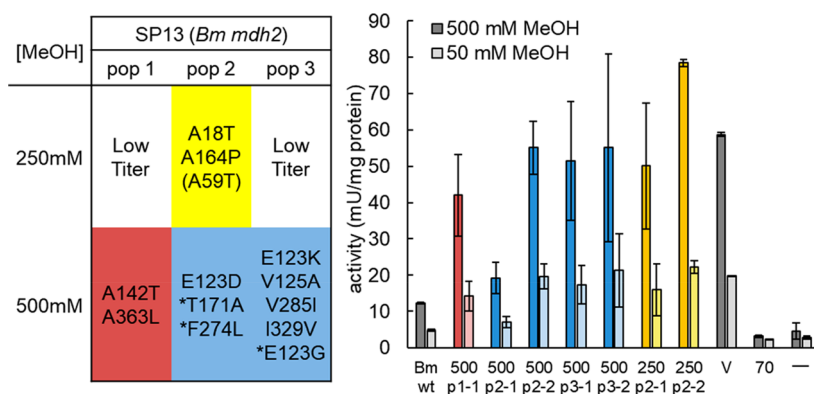
Figure 2. Four *Bm mdh2* populations emerging from PANCE contain variants that improve activity in cell lysate. (Left) Surviving populations after 38 passages evolved in the presence of 250 mM or 500 mM methanol. Within each population, all listed mutations were present in at least two sequenced individuals. Mutations in parentheses were present within a smaller subset of individuals containing the other listed mutation. Mutations preceded by an asterisk represent a separate set of converged mutations from those without asterisks. (Right) Crude lysate assays on isolated individuals from each surviving population show general improvements in activity *in vitro* for all converged genotypes. Darker bars show assays in the presence of 500 mM MeOH, while lighter bars show assays in the presence of 50 mM MeOH. Bars show the average of two biological replicates, while the top and bottom of error bars show each measured value. mCherry serves as a non-Mdh negative control. Activity is normalized to the total measured mg of protein in cell lysate. Variant "V" shows a representative M163V variant from the first PANCE experiment for comparison. Variant "70" shows a representative of passage 70 from the first PANCE experiment. A negative control strain expressing mCherry in place of Bm Mdh2 is shown as "—". The genotypes of assayed clones are listed in Table S1.
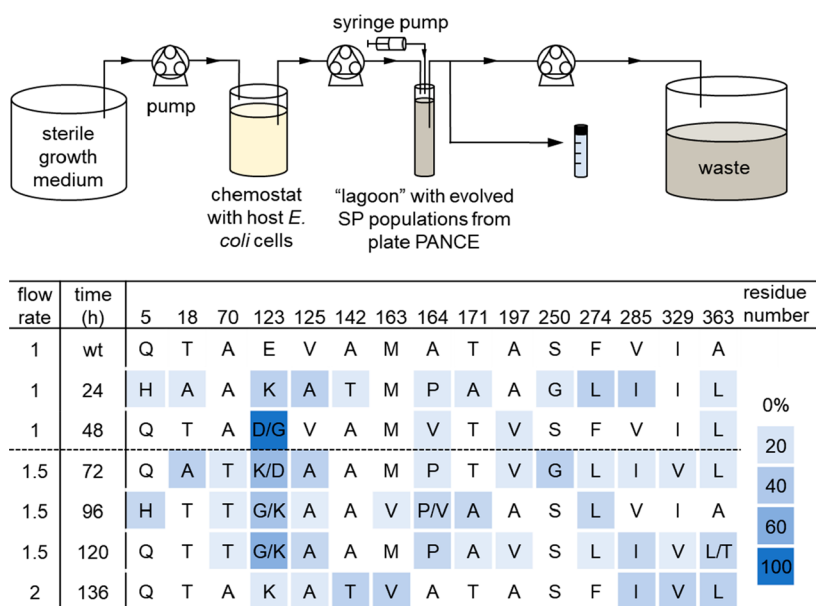

Figure 3. PACE of PANCE-evolved Mdh2 populations converges on variants that bind directly to FrmR. (Top) Overview of PACE. A constant volume evolving population of SP is maintained in the "lagoon", analogous to the evolving passages in PANCE. The syringe pump adds arabinose (10 mM final concentration), glutathione (5 mM), and methanol (125–250 mM) directly to the lagoon. (Bottom) Sequencing data for a PACE experiment seeded with plate-based PANCE populations. Flow rate is in lagoon volumes per hour. The dotted line shows where methanol concentrations were decreased from 250 to 125 mM methanol. The heat map indicates the percentage of sequenced individuals containing each mutation. Only coding mutations observed in at least three independent clones across all time points are shown. If no mutation was observed, the cell is colored white with the wild-type residue listed.

Sequencing of passage 38 phage revealed abundant Mdh2 mutations within each population, but with little similarity between the mutations in different PANCE culture wells evolved under the same conditions. Additionally, individuals within each population frequently contained different sets of mutations (Figure S3), similar to the results from passage 38 from the initial PANCE experiment (Figure S2), although none of the major genotypes in the plate selection contained the mutations from the single-culture selection. While the M163V mutation appeared in one clone in one of the populations evolved in the presence of 500 mM methanol, this mutation did not spread throughout the population and was not observed in other PANCE populations.

We focused our analysis on the four phage populations that exhibited the highest phage titers (>10^6 pfu/mL) after 38 PANCE passages (Figure 2). Among the new, predominant mutations, A164P was notable as adjacent to M163V and homologous to the critical A169 mutation reported in the evolution of Cn mdh2 CT4−1.[36] All but one of the clones containing the most abundant mutations in each PANCE well

showed at least a 2-fold increase in apparent Mdh2 activity in crude lysate assays compared to wild-type activity, with the A164P containing variant showing roughly 6-fold higher activity (Figure 2). Comparatively, a Q5L M163V clone representing the major outcome of the first PANCE experiment performed in culture tubes showed a 4.5-fold increase in activity, consistent with the improvements observed in the plate-based evolution. The fold increase in crude lysate assays was significantly lower than the apparent increase in luciferase assays, implying that there could be other factors that impact the *in vivo* activity of these variants. Nevertheless, the crude lysate activities clearly show that these mutations are not merely artifacts of the FrmR reporter system, but instead reflect improvements to the *in vitro* kinetic parameters of these mutants. Together, these results suggest that PANCE using miniaturized, multiplexed, plate-based replicate populations can rapidly provide access to Mdh2 mutations that increase apparent activity.

PACE of Bm Mdh2 PANCE Variants. Next, we combined separate PANCE populations together in one PACE experiment to determine if a more active evolved Mdh2 variant would emerge. We increased the stringency of the selection by switching to PACE and infected our lagoon with equal volumes of every methanol-treated population from passage 39 of our plate-based PANCE (Figure 3). We measured high phage titers for this lagoon in methanol concentrations as low as 125 mM methanol and at flow rates as high as 2.0 lagoon volumes per hour, which exceeded the stringency of the PANCE conditions used previously both in dilution rate and in methanol concentration. The survival of phage under these PACE conditions implied that Mdh2 populations could now survive under conditions that were not permissive for phage propagation when using wild-type Mdh2 as input. DNA sequencing revealed a mixture of genotypes mostly observed in the input PANCE populations, with only three new mutations (Q5H, A70T, and A197V) appearing in three or more sequenced clones. PANCE sampled many other coding mutations, but none that became predominant within the population. Additionally, two mutations observed during PANCE (S250G and M163V) appeared to enrich during PACE. Most notably, the M163V mutation was seen after the methanol concentration was decreased to 125 mM. The Q5L M163V variant from our first PANCE experiment provided a similar increase in Mdh activity in cell lysate as the other variants from the plate-based PANCE experiment used as input for PACE, and its presence in the PACE experiment suggests that it has a similar fitness to the rest of the PANCE. (Figure 2) These results collectively suggest that both PANCE and PACE evolved a variety of Mdh2 mutations that increased selection fitness (Figure 3).

Evolution at Low Methanol Concentrations Leads to FrmR-Binding Mdh Variants. While PACE took place at methanol concentrations as low as 125 mM, our first PANCE experiment showed strong propagation at 62.5 mM methanol (Figure 1). Mutations emerging from PANCE at 62.5 mM methanol, however, had strong activity in FrmR reporter assays even in the absence of methanol (Figure S4) despite showing no activity in cell lysate (Figure 2). We speculated that this phenotype was due either to a direct interaction between the mutant Mdh2 and the FrmR repressor, bypassing the methanol oxidation requirement, or to production of an off-target aldehyde that could interact with FrmR similarly to formaldehyde. In an effort to avoid propagating clones that would derepress FrmR from gene III and provide propagation in the absence of methanol oxidation, we designed a negative selection phase based on the gene III-neg system[9] to augment the existing selection and drift phases in PANCE.

The gene III-neg system consists of a plasmid almost identical to the standard FrmR-regulated AP, but instead of encoding gene III it encodes a dominant negative gene III variant that produces nonviable progeny in response to FrmR derepression in the absence of methanol (Figure S5). Phage that do not trigger the FrmR response are provided with gene III constitutively from a separate plasmid and propagate normally. As a result, the negative selection phase preferentially propagates phage that do not trigger the FrmR response in the absence of methanol over those that do (Figure S5),[3,9] in principle removing "cheater" Mdh2 mutants that cause FrmR derepression in a methanol-independent manner. To further limit the evolution of undesired phenotypes, we switched from using ethanol as a carrier for our chloramphenicol antibiotic during positive and drift selections (which results in a final ethanol concentration of 12 mM, likely competing with methanol for Mdh binding) to using DMSO, which has no known crosstalk with Mdh. We retained the ethanol during negative selection to penalize any possible effects of ethanol oxidation on the FrmR circuit. We used up to three negative selection phases with no methanol between selection phases with 125 or 62.5 mM methanol (Figure S6), but the dominant evolved variants we tested from the 62.5 mM selection phases still showed a strong FrmR response in the absence of methanol (Figure S7), suggesting that the fitness benefit of passing the selection phase at low methanol concentrations overcomes the fitness penalty of FrmR response during the negative selection phase.

To test whether or not methanol-independent FrmR derepression resulted from direct interaction between Mdh variants and FrmR, we cloned a variant of our AP that encodes a FrmR C35S mutant, which lacks the reactive cysteine required for formaldehyde response.[41−43] Because FrmR requires condensation of C35 with a reactive aldehyde species in order to change conformations and release its cognate DNA target,[42,43] we assumed that derepression of FrmR C35S would rule out oxidation of off-target substrates (*e.g.*, ethanol) as a mechanism for cheating the selection. The mutations that fixed first in the PANCE experiment (Q5L, M163V, and E180), and which persisted in all Bm Mdh2 cheater variants, do not derepress FrmR C35S on their own. However, two of the major genotypes isolated from the end of negative selection PANCE showed strong derepression of FrmR C35S (Figure S7), suggesting that the evolved cheater variants bind directly to FrmR. While one variant showed a slight increase in wild-type FrmR response upon addition of methanol, the other showed the same degree of derepression regardless of added methanol, suggesting that methanol oxidation no longer contributes to FrmR response for these cheaters. All other dominant variants from evolutions at 62.5 mM methanol similarly derepress FrmR C35S (Figure S8), suggesting that PACE and PANCE of Mdh2 at these lower concentrations preferentially leads to this undesirable phenotype rather than improved methanol oxidation.

Evolved Bm Mdh2 Variants Show Improved Activity in Vitro. Despite the evolution of some FrmR-binding Mdh2 variants, mutations at E123, M163, A164 and A363 improve bona fide Mdh activity (Figure 4) and were all observed among various genotypes emerging from PACE. However, none of
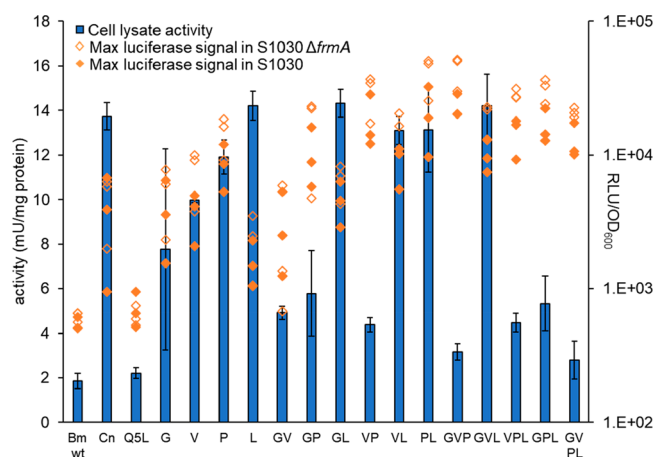
Figure 4. Cell lysate and luciferase reporter assays for Bm mdh2 variants with combined mutations. Diamonds show the maximum luminescence signal observed during continuous measurements taken for 4 h after induction of Mdh and addition of methanol to log-phase cultures in DRM. Separate diamonds for each strain show biological replicates measured across separate experiments. Filled diamonds = S1030; empty diamonds = S1030 $\Delta frmA$. Bars show the average of crude lysate *in vitro* activity assays for two replicates, while the top and bottom of error bars show each measured value. RLU = relative luminescence units; OD_{600} = optical density at 600 nm. All activities were measured in the presence of 50 mM methanol. G, V, P, and L stand for the mutations E123G, M163V, A164P, and A363L, respectively.

these mutations occurred simultaneously in the same variant. Wu and co-workers previously observed that higher activities could be achieved by manually recombining individual mutations emerging from a high-throughput screen for Cn Mdh2 variants.[36] To test if a combination of our independent Bm Mdh2 mutations would similarly improve activity, we manually cloned every possible single mutant and combination into a shared Q5L E180 background and compared their activity in both crude lysate and luciferase reporter assays (Figure 4). Every individual mutation we tested in this background showed improved activity over wild-type in both reporter and cell-lysate assays, with A164P having the highest increase in luciferase reporter assays (over 10-fold higher than wild-type at 50 mM methanol) and A363L having the highest crude lysate activity (over 7-fold higher than wild-type at 50 mM methanol). While the luciferase reporter assay data suggested that some of these single mutations in combination may have a slight improvement in activity (less than a 2-fold further improvement in relative luminescence signal), crude lysate data suggested that, in general, the A164P and A363L mutations on their own provided the best activity improvements. In crude lysate assays, recombining these two best-performing mutations with each other or E123G/M163V either has no apparent effect on activity compared to each individual mutation or significantly reduces activity, suggesting a negative epistatic interaction. In contrast, the reporter assays showed these combinations as generally better than individual mutants, particularly for A363L. None of these variants showed activity when no methanol was added to the culture, and similarly showed no activity when using a FrmR C35S reporter at any methanol dose (maximum signal for all tested strains was below 800 RLU/OD$_{600}$), suggesting that other factors are responsible for the disproportionate FrmR response. It is worth noting that the lysate assays were performed at a pH 9.5

following literature precedent.[33,36] Previous Mdh characterizations typically show a higher activity for Bm Mdh2 at this pH compared to the presumed pH of the *E. coli* cytoplasmic environment (7.4).[44] However, the variants carrying multiple mutated residues may have a stability trade-off not observed under physiological conditions that limits their activity at higher pH.

To further characterize these mutations, we purified N-terminal His-tagged Mdh2 variants carrying each of the single mutations tested as well as the combination mutant with the highest luciferase reporter signal for *in vitro* characterization (A164P A363L) and determined their Michaelis−Menten kinetic parameters (Table 1). Despite observing that the

Table 1. Kinetic Parameters for Evolved Bm Mdh2 Enzymes[a]

enzyme	$V_{\text{max,MeOH}}$ (mU/mg)	$K_{\text{m,MeOH}}$ (mM)	$k_{\text{cat}}/K_{\text{m}}$ (s^{-1} M^{-1})
Bm Mdh2 (wt)	36.5 ± 1.7	636 ± 74	0.23
Bm Mdh2 Q5L E123G	38.8 ± 1.6	615 ± 66	0.25
Bm Mdh2 Q5L M163V	55.0 ± 3.1	627 ± 89	0.35
Bm Mdh2 Q5L A164P	75.4 ± 2.3	440 ± 39	0.69
Bm Mdh2 Q5L A363L	127 ± 3.3	432 ± 32	1.18
Bm Mdh2 Q5L A164P A363L	88.5 ± 2.3	329 ± 28	1.08
Cn Mdh2 CT4−1	106 ± 2.1	88.8 ± 7.8	4.77

[a]Values are based on Michaelis−Menten fit for the data sets shown ± the asymptomatic standard error. mU/mg = milliunits per milligram of enzyme, with 1 unit defined as producing 1 μmol NADH per minute.

E123G variant was not substantially improved over wild-type, we measured up to a 3.5-fold higher V_{max} for all other evolved mutants compared to wild-type Bm Mdh2. Surprisingly, while the K_{m} of Bm Mdh2 seemed the most likely candidate for improvement given its high value (636 mM), the largest improvement was seen in the A164P A363L double mutant, which showed only a 1.9-fold improvement over wild-type (329 mM). While this K_{m} value was lower than either the A164P or A363L mutations on their own, the A363L single mutant still had a higher V_{max} value (Table 1), corroborating our previous cell lysate data (Figure 4).

Next, we compared our evolved variants to the state-of-the-art Cn Mdh2 CT4−1. While Cn Mdh2 CT4−1 still showed at least 3.7-fold lower K_{m} than any Bm Mdh2 variant, consistent with previous *in vitro* characterizations,[33,34,36] we observed a 1.2-fold higher V_{max} (127 mU/mg) for Bm Mdh2 Q5L A363L compared to Cn Mdh2 CT4−1 (106 mU/mg) (Table 1), although the $k_{\text{cat}}/K_{\text{m}}$ of Cn Mdh2 remains 4-fold higher than our best variant (4.77 s^{-1} M^{-1} for Cn Mdh2 CT4−1 *vs* 1.18 s^{-1} M^{-1} for Bm Mdh2 Q5L A363L). Compared to the evolution of Cn Mdh2 CT4−1, which improved *in vitro* activity largely through a significant decrease in K_{m} via a key A169V mutation,[36] our results suggest potential importance of these mutations in altering the rate of methanol oxidation rather than altering substrate binding to the enzyme. Surprisingly, the A164P variant is mutated at a homologous residue to the A169V variant reported by Wu and co-workers, which for Cn Mdh2 provides a significant reduction to K_{m}. further implicating the importance of this residue in the activity of these enzymes. Together, these results imply that the high K_{m} of Bm Mdh2 is not the only limiting factor in its activity. The lower K_{m} of Cn Mdh2 compared to the evolved Bm Mdh2

variants suggests that there may be further room for improvements *via* additional active site mutations, but as seen in the A164P A363L double mutant these improvements may come at the expense of V_{max}.

One of the key differences between Cn Mdh2 and Bm Mdh2 is the former's reported lack of activation by nudix hydrolases such as *Bacillus methanolicus* activator protein (Bm Act).[36] We determined whether or not our evolution impacted the *in vitro* activation previously observed for Bm Mdh2[44] by purifying Bm Act and testing the variants in Table 1 for methanol oxidation in the presence or absence of added Bm Act (Figure S9). As expected, we saw a strong (7.5-fold) improvement in wild-type Bm Mdh2 activity after the addition of Bm Act, whereas Cn Mdh2 CT4−1 showed a much lower (2.4-fold) activation. The evolved Bm Mdh2 variants showed lower activation than the wild-type, but still far more activation (4.6 to 5.6-fold) than Cn Mdh2 CT4−1. The general trend of lower activation suggests that further evolution of Bm Mdh2 could enable additional activator independence. Alternatively, recent work by Wang and co-workers published during the review of this manuscript shows that overexpression of the native *E. coli* Act homologue NudF can significantly improve methanol consumption in *E. coli* expressing both Bm Mdh1 and Bm Mdh2.[45] This contribution of NudF could possibly explain the similar activities of Bm Mdh2 variants and Cn Mdh2 CT4−1 in our cell lysate assays despite the superior kinetics of purified Cn Mdh2 CT4−1, despite previous work on wild-type Bm Mdh2 activation in *E. coli* cell lysate suggesting little-to-no major contribution from any such factors at their native expression levels.[30] Further research will be required to fully determine the impact of Act homologues on Mdh activity *in vivo*, and future evolution of Mdh in *E. coli* should consider the contribution of these factors toward activity. While there is likely room for further improvement of these enzymes both through strain engineering and further evolution, these data together validate PANCE as an effective way to access a variety of mutations that can improve the kinetic parameters of Bm Mdh2.

Homology Models Reveal a Common Region for Key Bm Mdh2 Mutations. To better understand why our individual evolved mutations improve activity individually, but not consistently when used in combination, we constructed a homology model of Bm Mdh2 with close alcohol dehydrogenase homologues using the Phyre 2 software developed by Kelley *et al.*[46] Bm Mdh2 has strong (>50%) sequence identity with several alcohol dehydrogenases. We aligned our homology model to the NAD⁺-bound structure of *Zymomonas mobilis* ZM4 ADH2 alcohol dehydrogenase[47] to approximate the location of the NAD⁺ molecule within the active site of our model (Figure 5). All key PANCE- and PACE-evolved mutated residues are predicted to localize to the same region proximal to the NAD cofactor binding pocket on this model, close to the expected redox-active region of the cofactor (Figure 5). Interestingly, E123, M163, and A164 all localize to one domain, while A363 localizes to a second domain on the other side of this binding pocket. Residues associated with cheater mutations conversely map away from the active site on the outer face of the domain containing the E123, M163 and A164 mutations, consistent with their ability to directly bind FrmR. Site-saturation mutagenesis of these residues and other residues near them may represent a promising strategy to further improve Bm Mdh2, and the similarity of these residues to the improvements seen in Cn
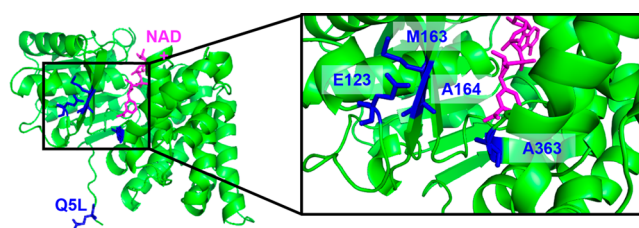

Figure 5. Mapping representative mutations in Bm mdh2 suggests possible mechanisms of improvement. Alignment of a Bm Mdh2 homology model to the highly similar *Zymomonas mobilis* alcohol dehydrogenase 2 (ZM4 ADH2) enables prediction of the NAD-binding region.[47,48]

Mdh2 suggests that other methanol dehydrogenases may also benefit from targeted mutagenesis within this region.

Evolved Bm Mdh2 Variants Outperform a State-of-the-Art Variant for *in Vivo* Methanol Assimilation. Finally, we tested whether our evolved Mdh variants could improve methanol assimilation in *E. coli*. We previously showed that during xylose/methanol cofeeding, Mdh kinetics limit ¹³C-methanol assimilation into central metabolism, even with evolved Cn Mdh2 CT4−1.[32] We compared the most improved *in vitro* variants to both the wild-type Bm Mdh2 and Cn Mdh2 CT4−1 using the same experimental setup and plasmid architecture as in our previous study.[32] All of the assayed evolved variants incorporated approximately twice as much methanol into central metabolites compared to both wild-type Bm Mdh2 and Cn Mdh2 CT4−1 (Figure 6). Interestingly, wild-type Bm Mdh2 performed as well as Cn Mdh2 CT4−1 despite the large disparity in their *in vitro* activities. The reasons for the discrepancy between *in vitro* activity and pathway efficacy for these two enzymes is currently unclear, but may arise from more efficient expression and solubility, factors that would not have greatly influenced the *in vitro* kinetics assays. These results show the viability of PANCE selections for evolving mutations that improve Mdh activity not just *in vitro*, but also for use in methanol assimilation pathways *in vivo*.

DISCUSSION

In five separate evolved populations, we observed distinct mutations that each improve Bm Mdh2 activity but are still insufficient to support synthetic methylotrophy in *E. coli* given our inability to grow strains expressing these variants using methanol as the sole carbon source. Further activity improvements might be achieved by increasing the stringency of our selection conditions, but lower methanol concentrations in our selections resulted in takeover by FrmR repressor-binding cheater variants. Given the high K_m values of the dehydrogenases characterized, gaining the ability to run our selections at lower methanol concentrations using selection techniques like fluorescence-activated cell-sorting (FACS) may allow researchers to more directly cull cheaters from an evolving population. Alternatively, further increasing the throughput of plate-based PANCE, for example using robotics platforms, could allow for a broader range of conditions to be tested to better avoid the rise of cheaters.

The results from this study, together with the homology models described above, provide a clearer picture of which residues are poised to impact activity of a given alcohol dehydrogenase with high sequence homology to Cn Mdh2 and Bm Mdh2. These developments thus make structure-driven
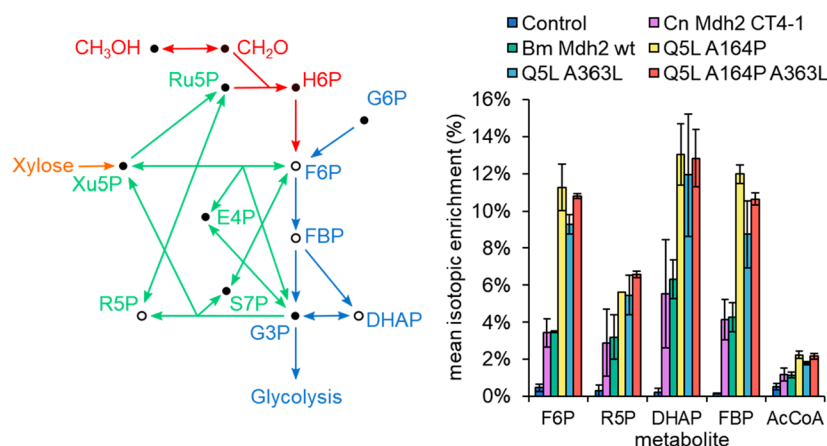
Figure 6. Improved ^{13}C-labeled methanol feedstock incorporation by evolved Bm mdh2 compared to the state-of-the-art methanol dehydrogenase. (Left) Metabolic network map showing the path of ^{13}C-labeled methanol through hps-phi and subsequent assimilation into central metabolism. Red lines show assimilation pathway reactions, blue lines show glycolysis reactions, and green lines show pentose-phosphate pathway reactions. Empty circle nodes and corresponding metabolites downstream of formaldehyde were measured metabolites in labeling experiments. (Right) ^{13}C enrichment for assimilation pathways using different Mdh enzymes (or GFP as a negative control) under equivalent xylose-fed conditions. Values and error bars show the average and standard deviation across three biological replicates. F6P = fructose 6-phosphate; FBP = fructose 1,6-bisphosphate; R5P = ribose 5-phosphate; DHAP = dihydroxyacetone phosphate; H6P = D-arabino-3-hexulo-6-phosphate; G6P = glucose 6-phosphate; Ru5P = ribulose 5-phosphate; G3P = glyceraldehyde 3-phosphate; E4P = erythrose 4-phosphate; S7P = sedoheptulose 7-phosphate; Xu5P = xylulose 5-phosphate.

rational engineering approaches an attractive alternative strategy for further Mdh engineering. Beyond methanol dehydrogenases, our work demonstrates the feasibility of PANCE for future metabolic enzyme evolution efforts, provided that appropriate care is taken to prevent intercellular diffusion of target molecules. While our approach used an extracellular chemical sink to sequester a reactive, diffusible molecule, not all metabolic products will have the required properties to take this approach. Other methods such as transporter knockouts or intracellular sequestration in polymers or inclusion bodies might be used to similar effect depending on the desired target activity. The 96-well PANCE format allows high-throughput protein evolution with minimal infrastructure requirements, providing an attractive alternative to more expensive, specialized platforms such as robotics-enabled high-throughput screens or FACS.

MATERIALS AND METHODS

Reagents. Unless specified, all chemical reagents were purchased in the highest grade available from Sigma−Aldrich. For luciferase reporter assays, M9 salts and LB, 2xYT, Agar, and casamino acids were purchased from US Biological Life Sciences. Trace Elements (MD-TMS) and Vitamin Solution (MD-VS) were purchased from ATCC. Antibiotics and Arabinose were purchased from GoldBioTechnology Inc.

Strains and Plasmids. Invitrogen Mach 1 T1R (Invitrogen) or NEB Turbo (NEB) chemically competent *E. coli* strains were used as cloning hosts. Luciferase reporter assays, phage-based assays, and all evolutions were carried out using *E. coli* S1030.[9] The original plasmid containing the *C. necator phaABCP* cassette from which the SP21 *phaC*-encoding SP was cloned (pMC001579) was gifted by Michelle Chang's Research group at University of California Berkeley. pETM6-mCherry was a gift from Mattheos Koffas (Addgene plasmid #66534).

Cloning. Plasmids and selection phage were constructed using USER cloning or KLD Enzyme Mix (NEB, Ipswich, MA). DNA fragments were generated by PCR using Pfu Turbo

Cx Hotstart DNA Polymerase (Agilent), VeraSeq 2.0 High Fidelity DNA Polymerase (Enzymatics), or Phusion U Hot Start DNA Polymerase (Thermo Fisher Scientific). All amplicons were purified using kits from Qiagen and digested with DpnI during PCR fragment assembly for USER cloning. All restriction endonucleases and USER enzyme were purchased from NEB. Assembled vectors were transformed into chemically competent *E. coli* of various strains and verified by Sanger sequencing after amplification from individual colonies using Illustra TempliPhi DNA Amplification kits (GE Healthcare). Cell growth for cloning purposes was carried out using 2xYT media supplemented with appropriate antibiotics (Kanamycin, 50 μg/mL; Carbenicillin, 50 μg/mL; Spectinomycin, 100 μg/mL). For phage cloning and replication, phage were transformed directly into S1059, S1381 or an equivalent phage containing a PSP-gene III plasmid (*e.g.*, pJC175e or similar)[9] and grown overnight. All transformed phage cultures were then plated on lawns of this same strain and individual plaques were picked into fresh media, grown for a minimum of 6 h, and verified by Sanger sequencing after amplification using Illustra TempliPhi DNA Amplification kits (GE Healthcare).

Luciferase Reporter Assays. For all reporter assays, the desired number of individual colonies from transformation plates were grown overnight at 37 °C in Davis Rich Media (DRM)[8] supplemented with carbenicillin (50 μg/mL from 1000× aqueous stock solution) and spectinomycin (100 μg/mL from 1000× aqueous stock solution). Cultures were diluted 100 to 1000-fold into fresh medium supplemented with 40 ng/mL anhydrotetracycline (ATc) if needed for FrmR expression from the pTR47m4 reporter plasmid and grown until early exponential phase (OD$_{600}$ approximately 0.4). At this stage, arabinose was added to induce expression of Mdh from the P$_{BAD}$ promoter, with full induction assumed at 1−10 mM. For continuous monitoring of luminescence, 200 μL of sample were placed into a Corning black clear bottom 96 well plate and analyzed for optical density at 600 nm and luciferase activity at 37 °C on an Infinite Pro M1000 plate reader

(Tecan). For discrete time points, 150 μL of culture was transferred to the same plates at given times postinduction and measured the same way. All liquid cultures and continuous cultures during plate-reading were grown with regular shaking (200 rpm) or stirring.

Plaque Assays for Phage Titer Quantification. For plaque assays used to clone and titer phage, the desired host strain for plaquing was grown at 37 °C to late log-phase (OD$_{600}$ 0.6−1.2). 100 to 200 μL of host culture was infected with 10 μL of a phage dilution series and diluted into 1 mL of molten 0.75% (w/v) agar in 2xYT and immediately plated on 1.5% (w/v) agar in 2xYT media. Agar was cooled and set before plates were inverted and grown overnight at 37 °C.

PACE Experiments. PACE experiments were performed as previously described.[1−3,5−10] All chemostat and lagoon systems were maintained using Masterflex Digital Pump systems (Cole-Parmer) at fixed RPM values manually calculated to provide a desired flow-rate for the tube diameter used during the experiment. TSS chemically competent *E. coli*[49] S1030 were transformed with desired AP and MP and plated on 2xYT agar containing 0.5 to 2% glucose (w/v). A single colony was grown to saturation overnight at 37 °C in DRM containing appropriate antibiotics and diluted the next day 100- to 1000-fold into a chemostat at 37 °C containing 50−100 mL of Davis Rich Media supplemented with appropriate antibiotics for the AP/MP used (Carbenicillin, 50 μg/mL; Chloramphenicol, 40 μg/mL, all dissolved directly into growth media from solid salts). Once the chemostat reached an OD$_{600}$ of ~0.8−1.2, dilution was started and adjusted in order to best maintain this OD$_{600}$ range, which varied by host but typically fell in the range of 0.5−1.2 chemostat volumes per hour. Chemostat media was flowed into lagoons at a desired flow-rate. Lagoons were treated with 1 M arabinose solution to 10 mM final lagoon concentration pumped from a syringe pump (New Era Pump Systems) and 1.5 mL/h of a 5−20% methanol and glutathione solution from a second syringe pump to achieve desired final concentrations of 0.5 to 2% (v/v) methanol (125 mM to 500 mM) and 5 mM glutathione. Phage were injected into lagoons to start the evolution and collected from lagoon waste needles or waste lines at desired time points. Phage titers were determined by plaquing onto pJC175e-containing S1030 derivatives, typically S1381.

Sequencing data was collected by picking individual plaques into fresh media and growing overnight. Overnight cultures were spun down and the supernatant used as template material for rolling circle amplification using Illustra TempliPhi DNA Amplification kits (GE Healthcare). Sequences were determined by Sanger sequencing and results were aligned using SeqMan alignment software (DNAStar) and manually analyzed and recorded. All liquid cultures and were grown with continuous shaking (200 rpm) or stirring.

PANCE Experiments. TSS chemically competent *E. coli*[49] S1030 were transformed with desired AP and MP and plated on 2xYT agar containing 0.5 to 2% glucose (w/v) along with appropriate concentrations of antibiotics (Carbenicillin, 50 μg/mL from 1000× aqueous stock solution; Chloramphenicol, 40 μg/mL from 1000× ethanol stock solution). A single colony was grown to saturation overnight at 37 °C in DRM containing appropriate antibiotics and diluted the next day 100- to 1000-fold into fresh DRM. Cultures were grown to log-phase (OD$_{600}$ 0.3−0.6), treated with 10 mM arabinose to induce mutagenesis, the desired amount of anhydrotetracycline for a given passage (0 or 40 ng/mL unless otherwise indicated),

glutathione solution to a final concentration of 10 mM, and the desired amount of methanol (0 to 500 mM). Treated cultures were split into the desired number of either 2 mL cultures in single culture tubes or 500 μL cultures in a 96-well plate and infected with selection phage. Infected cultures were grown overnight at 37 °C and harvested the next day *via* centrifugation (20 000 rcf for 2 min for individual culture tubes, 3000 rcf for 10 min for 96-well plates). Supernatant containing evolved phage was isolated with optional filtration through a 0.2 μm Costar spin filter (Corning) and stored at 4 °C. Isolated phage were then used to infect the next passage and the process repeated for however many passages were desired for the selection. Phage were diluted passage to passage a maximum of 10-fold and a minimum of 1000-fold. Phage titers were determined by plaquing onto pJC175e-containing S1030 derivative strain S1381. Sequencing data was collected by picking individual plaques into fresh media and growing overnight. Overnight cultures were spun down and the supernatant used as template material for rolling circle amplification using Illustra TempliPhi DNA Amplification kits (GE Healthcare). Sequences were determined by Sanger sequencing and results were aligned using SeqMan alignment software (DNAStar) and manually analyzed and recorded. All liquid cultures and were grown with continuous shaking (200 rpm) or stirring.

Crude Lysate Mdh Assays. TSS chemically competent *E. coli*[49] S1030 were transformed with desired pTR48 plasmid derivative encoding a given *mdh* gene and plated on 2xYT agar containing spectinomycin (100 μg/mL). Colonies were cultured overnight in DRM media containing spectinomycin (50 μg/mL), then diluted 100-fold into fresh media in the morning and incubated with shaking (200 rpm) at 37 °C until OD$_{600}$ 0.5−0.6. Mdh expression was induced with 10 mM arabinose, and growth continued for another 2 h. Cells were harvested by centrifugation (20 000 rcf, room temperature, 5 min), washed once with PBS, and the pellets frozen at −20C. Lysis was achieved with B-PER complete (0.1 mL B-PER per 1 mL culture, room temperature, 15 min), and the soluble fraction isolated by centrifugation (20 000 rcf, 4 °C, 20 min) and stored on ice until used. Methanol dehydrogenase activity was measured by following the methanol-dependent reduction of NAD$^+$ at 340 nm in 250 μL final volume using a clear, flat-bottom 96 well plate and SpectraMax model M2e plate reader with SoftMax Pro 6.5 software. The assay consisted of 100 mM glycine-KOH (pH 9.5), 5 mM MgSO$_4$ and 1 mM NAD$^+$, and was initiated by the addition of methanol to a final concentration of 50 mM or 500 mM. Product formation at 37 °C was quantified in comparison to a NADH standard curve. Total protein concentration in crude lysate was determined by Pierce BCA Assay (ThermoFisher). Activities are reported as arbitrary units, with one unit defined as 1 μmol NADH per minute, and normalized to total lysate protein concentration.

Mdh Purification. pET vectors encoding 6x-His-Mdh genes were transformed into BL21* (de3) Chemically Competent *E. coli* (Invitrogen) and plated on LB Agar with 50 μg/mL kanamycin at 37 °C. A single colony of each variant was inoculated into 2 mL of LB media with 50 μg/mL kanamycin and grown overnight at 37 °C. Overnight cultures diluted 1000-fold into to 200 mL of LB with 50 μg/mL kanamycin, 20 mM MgSO$_4$, and 100 μM ZnCl$_2$ and grown to OD$_{600}$ 0.6−1.2, induced with 0.1 mM IPTG, and grown overnight at 22 °C (220 rpm). Cultures were spun down at

10 000 rcf for 15 min at 4 °C, decanted, and resuspended in 3 mL B-PER reagent treated with EDTA-free protease inhibitor (Roche cOmplete, Mini, EDTA-free) and left at room temperature for 30−60 min. Lysed cells were spun down for 20 min at 20 000 rcf at 4 °C. Soluble lysate was decanted directly onto 2.5 mL of Ni-NTA resin (5 mL of a 50% solution washed with PBS, pH 7.4 with 10 mM imidazole to remove all ethanol). Flow through was collected by gravity and/or light application of vacuum to speed up the initial flow. The column was then washed with 2 to 10 mL of ice cold wash buffer (PBS pH 7.4 with 25 mM imidazole), followed by elution with 2 mL ice cold elution buffer (PBS pH 7.4 with 250 mM imidazole). Elution fractions were checked *via* SDS-PAGE gel, pooled, and transferred to Amicon 3 kDa CO Spin Columns and concentrated. Proteins were exchanged a total of 5 times into Tris-HCl (pH 7.5) to remove imidazole before overnight storage at 4 °C and kinetics analysis the following day, with a final estimated imidazole concentration of no more than 1 mM. Final protein concentrations were determined *via* Pierce BCA Protein Assay (ThermoFisher). One μg of each enzyme was analyzed *via* SDS-PAGE using a Bolt 4−12% Bis-Tris Plus Gel (ThermoFisher) and visualized with Instant Blue stain (Expedeon) to verify the purity and size of each enzyme. Enzyme not used for kinetics assays within 24 h was flash-frozen in liquid nitrogen and stored at −80 °C.

Mdh Kinetics. 1 mM NAD$^+$ was added to reaction buffer (100 mM glycine-NaOH (pH 9.5), 50 mM MgSO$_4$), and was incubated for 5 min with about 10 μg of Mdh enzyme at 37 °C. The methanol dehydrogenase reaction was initiated by the addition of methanol to a final concentration of 0, 10, 25, 50, 62.5, 125, 250, 500, 750, 1000, 1500, or 2000 mM at a final volume of 100 μL in a Corning black clear bottom 96 well plate. Product formation at 37 °C was quantified in comparison to an NADH standard curve prepared in reaction buffer. Total protein concentrations were reconfirmed by Pierce BCA Protein Assay (ThermoFisher). We note here that 50 mM MgSO$_4$ is ten times more concentrated than typical assay conditions, but this did not noticeably alter our observed reaction rates. Reactions were all blanked to a well containing reaction buffer with 1 mM NAD$^+$. Initial velocities were determined from the slope of a plot of the calculated concentration of NADH based on absorbance at 340 nm. Steady-state kinetic parameters were calculated by fitting these velocities to the Michaelis−Menten equation using the "fit" command in gnuplot (http://www.gnuplot.info/).

^{13}C Labeling and Analysis. Freshly transformed colonies of MG1655(DE3) $\Delta frmA^{32}$ were precultured overnight in Medium A (LB + 5 g/L xylose, 20 mM MgSO$_4$, 100 μM ZnCl$_2$, 50 μg/mL kanamycin from 1000× aqueous stock solution), then diluted 100-fold into fresh Medium A and incubated with shaking (200 rpm) at 37 °C until OD$_{600}$ 0.5−0.6. Pathway enzyme expression was induced with 100 μM IPTG, and growth continued for another 2 h. The culture was then centrifuged (10 min at 3500 rcf), washed once with an equal volume of M9 medium, and resuspended in an equal volume of M9 containing 5 g/L D-xylose, and 250 mM ^{13}C methanol (Cambridge Isotope Laboratories, 99%). Cells were incubated with shaking for a further hour before intracellular metabolites were extracted as described previously.[50] Briefly, 1 mL of liquid culture was filtered through a 0.45 μm nylon filter, washed with 10 mL room-temperature water, and then the filter was transferred into a 50 mL falcon tube containing 5 mL of extraction solution (40:40:20 acetonitrile:methanol:water)

at −20 °C. After 30 min, the filter was removed, the samples were centrifuged, and the supernatants dried overnight under air. The next morning, dried metabolites were resuspended in 150 μL water, centrifuged at 13 000 rpm for 40 min, and injected into an LC−MS/MS system as previously described.[50]

■ ASSOCIATED CONTENT

Ⓢ Supporting Information

The Supporting Information is available free of charge on the ACS Publications website at DOI: 10.1021/acssynbio.8b00481.

> Genotypes of evolved Mdh2 variants, additional luciferase reporter and cell lysate data for Mdh2 variants emerging from PANCE and PACE, descriptions of the negative selection and FrmR-binding Bm Mdh2 variants, and additional methods details (PDF)

■ AUTHOR INFORMATION

Corresponding Author
*E-mail: drliu@fas.harvard.edu.

ORCID Ⓘ
Gregory Stephanopoulos: 0000-0001-6909-4568
David R. Liu: 0000-0002-9943-7557

Author Contributions
#TBR and BMW contributed equally to this work.

Notes
The authors declare the following competing financial interest(s): The authors have filed patent applications on aspects of this work.

■ ACKNOWLEDGMENTS

■ ABBREVIATIONS

AP, accessory plasmid; SP, selection phage; MP, mutagenesis plasmid; DP, drift plasmid; PACE, phage assisted continuous evolution; PANCE, phage assisted noncontinuous evolution; ATc, anhydrotetracycline; Bm, *Bacillus methanolicus*; Cn, *Cupriavidus necator*; Mdh, methanol dehydrogenase.

■ REFERENCES

(1) Dickinson, B. C., Packer, M. S., Badran, A. H., and Liu, D. R. (2014) A system for the continuous directed evolution of proteases rapidly reveals drug-resistance mutations. *Nat. Commun. 5*, 5352.

(2) Packer, M. S., Rees, H. A., and Liu, D. R. (2017) Phage-assisted continuous evolution of proteases with altered substrate specificity. *Nat. Commun. 8*, 956.

(3) Bryson, D. I., et al. (2017) Continuous directed evolution of aminoacyl-tRNA synthetases. *Nat. Chem. Biol. 13*, 1253−1260.

(4) Suzuki, T., et al. (2017) Crystal structures reveal an elusive functional domain of pyrrolysyl-tRNA synthetase. *Nat. Chem. Biol. 13*, 1261−1266.

(5) Badran, A. H., et al. (2016) Continuous evolution of *Bacillus thuringiensis* toxins overcomes insect resistance. *Nature 533*, 58−63.

(6) Hubbard, B. P., et al. (2015) Continuous directed evolution of DNA-binding proteins to improve TALEN specificity. *Nat. Methods* 12, 939−942.

(7) Hu, J. H., et al. (2018) Evolved Cas9 variants with broad PAM compatibility and high DNA specificity. *Nature* 556, 57−63.

(8) Esvelt, K. M., Carlson, J. C., and Liu, D. R. (2011) A system for the continuous directed evolution of biomolecules. *Nature* 472, 499−503.

(9) Carlson, J. C., Badran, A. H., Guggiana-Nilo, D. A., and Liu, D. R. (2014) Negative selection and stringency modulation in phage-assisted continuous evolution. *Nat. Chem. Biol.* 10, 216−222.

(10) Dickinson, B. C., Leconte, A. M., Allen, B., Esvelt, K. M., and Liu, D. R. (2013) Experimental interrogation of the path dependence and stochasticity of protein evolution using phage-assisted continuous evolution. *Proc. Natl. Acad. Sci. U. S. A.* 110, 9007−9012.

(11) Mahr, R., and Frunzke, J. (2016) Transcription factor-based biosensors in biotechnology: current state and future prospects. *Appl. Microbiol. Biotechnol.* 100, 79−90.

(12) Khosla, C. (2009) Structures and Mechanisms of Polyketide Synthases. *J. Org. Chem.* 74, 6416−6420.

(13) Nielsen, J., and Keasling, J. D. (2016) Engineering Cellular Metabolism. *Cell* 164, 1185−1197.

(14) Schrader, J., et al. (2009) Methanol-based industrial biotechnology: current status and future perspectives of methylotrophic bacteria. *Trends Biotechnol.* 27, 107−115.

(15) Hanson, R. S., and Hanson, T. E. (1996) Methanotrophic bacteria. *Microbiol. Rev.* 60, 439−471.

(16) *Global Anthropogenic Non-CO2 Greenhouse Gas Emissions: 1990−2030.* US EPA (2016) https://www.epa.gov/global-mitigation-non-co2-greenhouse-gases/global-anthropogenic-non-co2-greenhouse-gas-emissions (accessed 30th March 2018).

(17) Elvidge, C. D., et al. (2009) A Fifteen Year Record of Global Natural Gas Flaring Derived from Satellite Data. *Energies (Basel, Switz.)* 2, 595−622.

(18) Fei, Q., et al. (2014) Bioconversion of natural gas to liquid fuel: Opportunities and challenges. *Biotechnol. Adv.* 32, 596−614.

(19) Clomburg, J. M., Crumbley, A. M., and Gonzalez, R. (2017) Industrial biomanufacturing: The future of chemical production. *Science* 355, aag0804.

(20) Conrado, R. J., and Gonzalez, R. (2014) Envisioning the Bioconversion of Methane to Liquid Fuels. *Science* 343, 621−623.

(21) Haynes, C. A., and Gonzalez, R. (2014) Rethinking biological activation of methane and conversion to liquid fuels. *Nat. Chem. Biol.* 10, 331−339.

(22) Quayle, J. R., and Ferenci, T. (1978) Evolutionary aspects of autotrophy. *Microbiol. Rev.* 42, 251−273.

(23) Peyraud, R., et al. (2009) Demonstration of the ethylmalonyl-CoA pathway by using 13C metabolomics. *Proc. Natl. Acad. Sci. U. S. A.* 106, 4846−4851.

(24) Müller, J. E. N., Heggeset, T. M. B., Wendisch, V. F., Vorholt, J. A., and Brautaset, T. (2015) Methylotrophy in the thermophilic Bacillus methanolicus, basic insights and application for commodity production from methanol. *Appl. Microbiol. Biotechnol.* 99, 535−551.

(25) Hu, B., and Lidstrom, M. E. (2014) Metabolic engineering of Methylobacterium extorquens AM1 for 1-butanol production. *Biotechnol. Biofuels*, DOI: 10.1186/s13068-014-0156-0.

(26) Marx, C. J., and Lidstrom, M. E. (2001) Development of improved versatile broad-host-range vectors for use in methylotrophs and other Gram-negative bacteria. *Microbiology (London, U. K.)* 147, 2065−2075.

(27) Marx, C. J., and Lidstrom, M. E. (2004) Development of an insertional expression vector system for Methylobacterium extorquens AM1 and generation of null mutants lacking mtdA and/or fch. *Microbiology (London, U. K.)* 150, 9−19.

(28) Schada von Borzyskowski, L., Remus-Emsermann, M., Weishaupt, R., Vorholt, J. A., and Erb, T. J. (2015) A Set of Versatile Brick Vectors and Promoters for the Assembly, Expression, and Integration of Synthetic Operons in Methylobacterium extorquens AM1 and Other Alphaproteobacteria. *ACS Synth. Biol.* 4, 430−443.

(29) Whitaker, W. B., Sandoval, N. R., Bennett, R. K., Fast, A. G., and Papoutsakis, E. T. (2015) Synthetic methylotrophy: engineering the production of biofuels and chemicals based on the biology of aerobic methanol utilization. *Curr. Opin. Biotechnol.* 33, 165−175.

(30) Müller, J. E. N., et al. (2015) Engineering Escherichia coli for methanol conversion. *Metab. Eng.* 28, 190−201.

(31) Meyer, F., et al. (2018) Methanol-essential growth of Escherichia coli. *Nat. Commun.* 9, 1508.

(32) Woolston, B. M., King, J. R., Reiter, M., Hove, B. V., and Stephanopoulos, G. (2018) Improving formaldehyde consumption drives methanol assimilation in engineered E. coli. *Nat. Commun.* 9, 2387.

(33) Krog, A., et al. (2013) Methylotrophic Bacillus methanolicus encodes two chromosomal and one plasmid born NAD+ dependent methanol dehydrogenase paralogs with different catalytic and biochemical properties. *PLoS One* 8, e59188.

(34) Whitaker, W. B., et al. (2017) Engineering the biological conversion of methanol to specialty chemicals in Escherichia coli. *Metab. Eng.* 39, 49−59.

(35) *EPA Method 8315A (SW-846): Determination of Carbonyl Compounds by High Performance Liquid Chromatography (HPLC).* US EPA (2015) https://www.epa.gov/homeland-security-research/epa-method-8315a-sw-846-determination-carbonyl-compounds-high-performance (accessed 28th March 2018).

(36) Wu, T.-Y., et al. (2016) Characterization and evolution of an activator-independent methanol dehydrogenase from Cupriavidus necator N-1. *Appl. Microbiol. Biotechnol.* 100, 4969−4983.

(37) Woolston, B. M., Roth, T., Kohale, I., Liu, D. R., and Stephanopoulos, G. (2018) Development of a formaldehyde biosensor with application to synthetic methylotrophy. *Biotechnol. Bioeng.* 115, 206−215.

(38) Badran, A. H., and Liu, D. R. (2015) Development of potent in vivo mutagenesis plasmids with broad mutational spectra. *Nat. Commun.* 6, 8425.

(39) Davis, J. H., Rubin, A. J., and Sauer, R. T. (2011) Design, construction and characterization of a set of insulated bacterial promoters. *Nucleic Acids Res.* 39, 1131−1141.

(40) Peoples, O. P., and Sinskey, A. J. (1989) Poly-beta-hydroxybutyrate (PHB) biosynthesis in Alcaligenes eutrophus H16. Identification and characterization of the PHB polymerase gene (phbC). *J. Biol. Chem.* 264, 15298−15303.

(41) Denby, K. J., et al. (2016) The mechanism of a formaldehyde-sensing transcriptional regulator. *Sci. Rep.* 6, 38879.

(42) Law, J. (2012) *Molecular Basis of Bacterial Formaldehyde Sensing,* University of Manchester.

(43) Osman, D., et al. (2016) The Effectors and Sensory Sites of Formaldehyde-responsive Regulator FrmR and Metal-sensing Variant. *J. Biol. Chem.* 291, 19502−19516.

(44) Ochsner, A. M., Müller, J. E. N., Mora, C. A., and Vorholt, J. A. (2014) In vitro activation of NAD-dependent alcohol dehydrogenases by Nudix hydrolases is more widespread than assumed. *FEBS Lett.* 588, 2993−2999.

(45) Wang, X., et al. (2019) Methanol fermentation increases the production of NAD(P)H-dependent chemicals in synthetic methylotrophic Escherichia coli. *Biotechnol. Biofuels* 12, 17.

(46) Kelley, L. A., Mezulis, S., Yates, C. M., Wass, M. N., and Sternberg, M. J. E. (2015) The Phyre2 web portal for protein modeling, prediction and analysis. *Nat. Protoc.* 10, 845.

(47) Moon, J.-H., et al. (2011) Structures of Iron-Dependent Alcohol Dehydrogenase 2 from Zymomonas mobilis ZM4 with and without NAD+ Cofactor. *J. Mol. Biol.* 407, 413−424.

(48) *The PyMOL Molecular Graphics System,* Version 2.0, Schrödinger, LLC.

(49) Chung, C. T., and Miller, R. H. (1993) Preparation and storage of competent Escherichia coli cells. *Methods Enzymol.* 218, 621−627.

(50) King, J. R., Woolston, B. M., and Stephanopoulos, G. (2017) Designing a New Entry Point into Isoprenoid Metabolism by Exploiting Fructose-6-Phosphate Aldolase Side Reactivity of Escherichia coli. *ACS Synth. Biol.* 6, 1416−1426.